RESEARCH ARTICLE

Deficient uracil base excision repair leads to persistent dUMP in HIV proviruses during infection of monocytes and macrophages

Mesfin Meshesha, Alexandre Esadze, Junru Cui, Natela Churgulia, Sushil Kumar Sahu, James T. Stivers *

Department of Pharmacology and Molecular Sciences, Johns Hopkins University School of Medicine, Baltimore, MD, United States of America

* jstivers@jhmi.edu

Abstract

Non-dividing cells of the myeloid lineage such as monocytes and macrophages are target cells of HIV that have low dNTP pool concentrations and elevated levels of dUTP, which leads to frequent incorporation of dUMP opposite to A during reverse transcription ("uracilation"). One factor determining the fate of dUMP in proviral DNA is the host cell uracil base excision repair (UBER) system. Here we explore the relative UBER capacity of monocytes (MC) and monocyte-derived macrophages (MDM) and the fate of integrated uracilated viruses in both cell types to understand the implications of viral dUMP on HIV diversification and infectivity. We find that the kinetics for MC infection is compatible with their lifetime *in vivo* and their near absence of hUNG2 activity is consistent with the retention of viral dUMP at high levels at least until differentiation into macrophages, where UBER becomes possible. Overexpression of human uracil DNA glycosylase in MDM prior to infection resulted in rapid removal of dUMP from HIV cDNA and near complete depletion of dUMP-containing viral copies. This finding establishes that the low hUNG2 expression level in these cells limits UBER but that hUNG2 is restrictive against uracilated viruses. In contrast, overexpression of hUNG2 after viral integration did not accelerate the excision of uracils, suggesting that they may poorly accessible in the context of chromatin. We found that viral DNA molecules with incorporated dUMP contained unique (+) strand transversion mutations that were not observed when dUMP was absent (G→T, T→A, T→G, A→C). These observations and other considerations suggest that dUMP introduces errors predominantly during (-) strand synthesis when the template is RNA. Overall, the likelihood of producing a functional virus from *in vitro* infection of MC is about 50-fold and 300-fold reduced as compared to MDM and activated T cells. The results implicate viral dUMP incorporation in MC and MDM as a potential viral diversification and restriction pathway during human HIV infection.

Introduction

A role for the uracil base excision repair (UBER) pathway in HIV-1 infection of non-dividing macrophage and monocyte immune cells has been of interest for many years in at least two

Competing interests: The authors have declared
that no competing interests exist.

different biological contexts. These contexts arise from two innate immune responses that
result in the introduction of dUMP into viral DNA [1–5]. These responses involve either enzy-
matic cytosine deamination of the viral (-) strand cDNA by APOBEC DNA deaminases [1,2]
or the incorporation of dUMP opposite to adenine on either strand of viral DNA during
reverse transcription [3,4,6]. The incorporation pathway arises specifically in quiescent cells
because [dUTP] is typically higher in such non-dividing cells and most DNA polymerases
readily utilize dUTP as a substrate in competition with dTTP [7–9]. The two uracilation path-
ways are quite unique because cytosine deamination leads to G>A transition mutations at spe-
cific trinucleotide sequences on (+) strand genomic RNA [10], while dUMP incorporation
opposite to adenine occurs on both strands and is not intrinsically mutagenic [3]. Previous
studies by us and others indicate that the majority of the dUMP that is present with *in vitro*
infected monocyte-derived-macrophages (MDM) arises from dUMP incorporation by reverse
transcriptase [4,6]. Once the viral DNA products enter the nuclear compartment, both types of
lesions are substrates for uracil excision by the enzyme nuclear uracil DNA glycosylase
(hUNG2) [3], the first enzyme in the UBER pathway. Excision by hUNG2 could lead to a vari-
ety of different outcomes ranging from viral DNA damage via strand breaks to replacement of
dUMP with dTMP, restoring canonical T/A pairs [4,6]. We have previously reported that HIV
DNA obtained from alveolar macrophages and circulating blood monocytes from drug naïve
and ART patients both contained high levels of dUMP, while T cells from the same patients
did not [4]. These findings suggest that uracilation occurs during *in vivo* HIV infection of both
macrophages and their monocyte precursors.

It is not clear how HIV-1 remains infective in the hostile deoxynucleotide pool environ-
ment of quiescent cells, where overall dNTP concentrations are low and the ratio of [dUTP]/
[TTP] is large [11,12]. One plausible explanation is that dUMP/A pairs are well-tolerated in
viral cDNA and persist due to very low hUNG2 activity in non-dividing MDM [4]. The intrin-
sically low activity of hUNG2 in these cells could be further reduced by the ubiquitin-mediated
degradation of hUNG2 facilitated by the HIV-1 accessory protein Vpr [4,13–15]. In addition
to promoting proteasomal degradation, Vpr has also been suggested to act as a transcriptional
repressor of hUNG2 [16]. Another possible outcome in the context of low hUNG2 expression
would be slow uracil excision, followed by repair. Over time, and after many excision/incorpo-
ration events, proviral dUMP would eventually be replaced with TMP, leading to canonical T/
A base pairs. Support for such a replacement mechanism was previously suggested because the
levels of dUMP in proviruses decreased over four weeks of culturing infected MDM [4]. The
persistence of dUMP in viral DNA and the slow replacement mechanism have implications
for viral latency in quiescent cells because *in vitro* and cellular transcription from uracilated
DNA templates is greatly reduced even in the complete absence of hUNG activity [9]. This
inhibitory effect of dUMP/A pairs arises at the level of transcription factor binding and RNA
pol II activity [9,17]. The complexity of this biology that is unique to quiescent cells, challenges
efforts to unravel the contributions of the component factors. Nevertheless, the fact that HIV-1
targets the UBER repair pathway at both the transcriptional and protein level indicates an evo-
lutionary pressure to diminish the activity of this pathway during infection [16].

In this study we further explore the nucleotide profiles and UBER activities of MDM and
their monocyte precursors with the aim of comparing the outcomes of dUMP incorporation
and UBER activity during infection of these cell types. The motivation for this work is the pre-
vious observation by us and others that HIV DNA is detected in circulating monocytes (MC)
and alveolar macrophages (AM) in patients receiving ART who test negative for HIV RNA in
blood samples (10–600 HIV copies have been detected per million MC or AM) [4,18,19].
Given that circulating MC are short-lived ($t_{1/2}$ ~ several days) [20], the detection of HIV DNA
in these cells of virus-free patients suggests that they arise from contact with latently infected

cells in one or more HIV drug-resistant reservoirs, possibly by passing through a compartment that contains infected resident macrophages (or T cells) and then re-entering circulation. Productively infected MC could then seed infection in new tissues [21–23]. We now report that MC are much more deficient in UBER activities compared to MDM such that high levels of viral dUMP persist during the entire lifetime of a circulating MC. When infected MC eventually differentiate into MDM, the existing proviral dUMP can be slowly replaced by TMP using the UBER activities present in MDM. The implications for human HIV infection and potential therapeutic opportunities arising from these findings are discussed.

Materials and methods

Cells

Monocytes (MC) were purified from peripheral blood mononuclear cells (PBMC) of HIV negative consenting donors under Johns Hopkins University IRB approval (IRB00038590) using a Ficoll-Hypaque density gradient followed by negative selection using a Pan monocyte isolation kit (Miltenyi Biotech). Monocyte purified by the pan monocyte isolation kit were checked for T-cell contamination by RT-PCR using TCR-β primer pairs which gave 99% purity (see detail in **S1 Methods**). In some cases, to prevent cell adherence and differentiation into monocyte-derived macrophages (MDM), MC were cultured up to 7 days in suspension using ultra-low adherence 96-well plates (Corning) using RPMI 1640 (Gibco) supplemented with 10% donor autologous serum, 100 μg/ mL penicillin, 100 μg/mL streptomycin (HyClone), 0.3 mg/ml glutamine and 10 mM HEPES (RPMI-AS). Fully-differentiated MDM were generated by culturing MC under adherent conditions for seven days using RPMI-AS medium supplemented with 10 ng/mL M-CSF (R&D Systems). T cells were purified from PBMC using T cell pan isolation kit (Miltenyi Biotec). T cells were first cultured for three days using stimulating conditions (RPMI supplemented with 10% (vol/vol) donor autologous serum, 100 μg/ mL penicillin, 100 μg/mL streptomycin (HyClone), 0.3 mg/ml glutamine 1 mg/ml of Phytohemagglutinin (Gibco) and, ciprofloxacin (5 μg/ml)). T cells were then infected with HIV^{BaL} and cultured for up to 7 days in RPMI medium additionally supplemented with 10 U/ml recombinant interleukin-2 (Sigma). The dividing cell lines HEK293T (ATCC) and Hap1 (Horizon Discovery) were seeded at 2 million cells per T-75 flask. The culture media for the dividing cells (HI-10) consisted of RPMI-1640 medium + 10% heat inactivated FBS (Sigma), 100 μg/mL penicillin and 100 μg/mL streptomycin. Cells were grown until 70% confluence with media changes every 48 h. The cells were released from the flask using 5 mL of 0.05% trypsin-EDTA (Gibco), followed by washing three times with PBS (Gibco) without CaCl$_2$ or MgCl$_2$.

Single nucleotide polymerase extension assay

Methanol extraction of total dNTPs from ~ 1–2 million cells and quantification of dUTP and dTTP were performed as previously described [3], except that HIV-1 reverse transcriptase (RTase) was used in the extension assay (Millipore-Sigma). Further details are described in the **S1 Methods**.

Western blotting

Extracts for western blotting were prepared using denaturing conditions with approximately 4 million MC or 2 million MDM that were collected from culture plates by treatment with trypsin. Further details are described in the **S1 Methods**.

Uracil DNA glycosylase activity assay

The hUNG activity present in cell extracts was measured using a molecular beacon fluorescent hairpin DNA substrate containing U/A base pairs as previously described [3,4]. The UNG activity was normalized to the total extract protein. The measured uracil excision activity was fully inhibited by the addition of uracil DNA glycosylase inhibitor protein (UGI) to the extracts, establishing that only hUNG and not any other glycosylase activity was being detected.

Activity of HIV reverse transcriptase with dUTP and dTTP substrates

To test whether dUMP is an efficient substrate for reverse transcription by HIV RTase, we measured its capacity to distinguish between dTTP and dUTP incorporation using the SNE assay described above. For these measurements we assembled two 100 μL reactions with dNTP mixtures consisting of 1200 fmol dCTP, dGTP, dATP and containing either dTTP or dUTP. The reactions contained 600 fmol of a 5′-FAM-labeled DNA template-primer with a single A overhang on the template strand. To these reactions 1 μL (2 units) of recombinant HIV RTase was added and incubated at 37 ^{0}C. Ten μL samples were removed at 0, 10, 20, 30, 60, 120, 240, 2400 s, quenched in 40 μL of 98% formamide containing 20 mM EDTA (pH 8.0), and resolved on a 15% denaturing polyacrylamide gel. The initial linear rates of dUTP or dTTP incorporation into the primer strand were measured by fitting data points at < 40% reaction.

Viruses and infections

The macrophage tropic replicative HIV-1 virus HXB3/BaL was obtained from the NIH AIDS Reagent Program (Catalog #11414) and propagated in MOLT-4/CCR5 cells. Culture supernatants of infected MOLT-4/CCR5 cells were collected at 12 to 15 dpi, centrifuged to clear cellular debris, passed through 0.45 μm filters, aliquoted, and stored at -80˚C. Vesicular stomatitis virus G protein (VSV-G) pseudo-typed HIV-1 virions (HIVNL4.3$^{(VSVG)}$) were generated as previously described (3) by co-transfection of HEK 293T cells with pNL4-3-ΔE-eGFP and pVSV-G. pCW57.1.FL.UNG lentiviral particles (LV) were generated by transfecting HEK 293 T cells with; 90 ug of pCW 57.1 hUNG, 90 ug of pMDLg/pRRE packaging plasmid (containing Gag & Pol, Addgene), 36 ug of pRSV-Rev packaging plasmid (containing Rev, Addgene), 18 ug of pMD2.g packaging plasmid (containing VSV-G envelope, Addgene). Transfection was performed using Lipofectamin 2000 (Invitrogen) following the manufacturers protocol. Lentivral particles were then concentrated over 20% sucrose cushion and ultracentrifugation at 28 k RPM for two hours. Viral titer was determined by the ELISA p24 antigen assay (Lenti-X p24 Rapid Titer Kit, TaKaRa). Monocytes were infected immediately after purification by adding HIV-1^{BaL} virus to the culture at MOI between 3 and 5 based on the p24 titer. After infection, monocytes were cultured in two different manners: (i) non-adherent growth conditions in the absence of M-CSF to minimize differentiation by adherence or cytokine mechanisms or, (ii) by adherent growth for seven days in the presence of M-CSF to promote differentiation into MDM over the infection. Infections of fully differentiated MDM were performed after adherent growth in the presence of M-CSF for seven days. Just prior to addition of virus to MDM, the media was replaced with RPMI + 10% dFCS and omitting M-CSF. Monocytes and MDM were also cultured in the presence of 5 mM thymidine (Sigma) overnight to increase the intracellular dTTP levels prior to infection with HIV-1^{BaL} ("thymidine rescue" conditions).

Viral copy number using qPCR and ddPCR

Viral copy numbers were determined using qPCR. A standard curve for viral copy number quantification was developed using 10-fold serial dilutions of DNA extracted from J-lat cells

that contain a single integrated HIV per genome (NIH AIDS Reagent Program). Real time qPCR was performed using a Qiagen Rotor-Gene qPCR instrument using the Rotor-gene Probe PCR kit. Reactions were performed in a 25 μl reaction volume using 0.4 μM forward and reverse primers and 0.2 μM of specific hydrolysis probes. PCR targeted the early or late HIV reverse transcripts (ERT or LRT). Amplification was performed using a two-step program: initial heating at 95 ^{0}C for five minutes, followed by 40 cycles of denaturation at 95 ^{0}C for 10 seconds and annealing and extension at 60 ^{0}C for 30 seconds. For determination of viral copies per cell, simultaneous quantification of the genomic RnaseP (RPP30) gene was performed using published primers and a specific probe as previously described [4]. All primers and probes used in this study are listed in S1 Table.

Determination of HIV proviral DNA using alu-gag nested PCR

To determine copy numbers of HIV proviral DNA, a nested PCR method was used [26]. The first PCR was performed using a forward primer that targeted genomic *alu* sequences randomly located near integrated proviruses (0.2 μM) and an HIV-specific *gag* reverse primer (1.2μM). Other PCR conditions were 200 μM of each dNTP, 1X LongAmp taq buffer (NEB), 5 units of LongAmp taq DNA polymerase (NEB) and 50 ng of DNA sample extracted from infected cells in a 50μl final reaction volume. Amplification was performed using the following thermocycler program: initial activation heating 94 ^{0}C for two min, followed by 20 cycles of denaturation at 94 ^{0}C for 30 sec, annealing at 50 ^{0}C for 30 sec and extension at 65 ^{0}C for three min and a final extension reaction at 65 ^{0}C for ten minutes. The PCR product is diluted 20-fold and five μl of the diluted PCR product is used as an input material for the second PCR reaction, which is performed using LRT forward and reverse primers and probe using the Rotor Gene Probe PCR kit (Qiagen) as described above. Proviral copy numbers were determined using the J-lat cell integration standard as described above. Genomic copy numbers were determined using the RPP30 qPCR measurement described above using the same amount of input total DNA sample used to measure proviral copy numbers.

Uracil content of viral DNA

Uracil content of viral DNA was determined using either uracil excision droplet digital PCR (Ex-ddPCR) or a similar qPCR method (Ex-qPCR) as previously described [4] with some modifications as described in the S1 Methods.

RT-qPCR of extracellular viral RNA

Culture supernatants were collected from infected MC, MDM^{EI} or MDM^{LI} 7-days post infection unless otherwise specified. Supernatants were first spun to remove cellular debris, filtered using 0.22 μm filter and frozen at -80 ^{0}C until use. RNA was extracted from 140 μl of culture supernatant using the Qiagen mini-Viral Prep kit according to the manufacturer's protocol. RNA (~3 μg) was treated with 2 units turbo-DNase (Invitrogen) in 1X turbo-DNase buffer for 30 min at 37˚C, to remove DNA carryover and then purified using Qiagen RNEasy kit. About 1.3 μg of RNA was used to generated cDNA with the Qiagen OmniScript cDNA preparation kit following the manufacturers protocol. Using the cDNA as input material and the Rotor Gene qPCR probe kit (Qiagen), the genomic HIV RNA copies in the supernatants of infected MC and MDM cultures were measured relative to a standard curve developed with the J-lat HIV integration standard cell line (see above). Thermal cycling conditions for qPCR consisted of 95˚C for 5 min, and 40 cycles of denaturation at 95˚C for 10 sec and annealing and extension at 60˚C for 30 sec. The measurements are reported as RNA copies per provirus present.

Sequencing of single viral reverse transcripts and genomic RNA copies

Monocytes and MDMs were infected with HIV-1^{BaL} as described above and culture extracts and supernatants were collected at 7 days post infection, filtered and frozen at -80˚C until use. A combination of qPCR and limiting-dilution PCR were performed to obtain samples that contained single copies of viral DNA and RNA as determined by the fraction of qPCR-positive samples at each dilution. Dilutions where one out of five replicates tested positive were taken as clonal according to Poisson statistics [4,9]. Amplified single copies were then sequenced by the Sanger method. Further details are described in **S1 Methods**.

ELISA measurements of viral p24

The Lenti-X p24 Rapid Titer Kit from TaKaRa was used following the manufacturer's protocol. Further details are provided in **S1 Methods.**

Infectivity of virus isolated from MC and MDM

MOLT-4/CCR5 target cells were infected overnight at an MOI of 0.5 (0.1 pg p24/cell) using HIV-1^{BaL} virus collected from three different producer culture supernatants: (i) MC infected immediately after isolation and cultured for 7 days under non-adherent conditions in the absence of M-CSF to maintain a monocyte-like phenotype, (ii) infected monocytes that were cultured for seven days in the presence of M-CSF [we refer to these cells as "*early infection*" macrophages (MDM^{EI}) to indicate that they were infected before differentiating into MDM], and (iii) MDM that were infected after differentiating for 7 days under adherent conditions in the presence of M-CSF [we refer to these infected cells as MDM^{LI}) to indicate that infection occurred after the macrophage phenotype was achieved]. One day after the addition of the virus to the MOLT-4/CCR5 cells, the cells were washed and cultured in RPMI 1640 (Invitrogen) supplemented with 10% heat inactivated bovine serum, 100 U/ml penicillin, 100 μg/ml streptomycin, 0.3 mg/ml glutamine and 200 μg/ml neomycin. DNA was extracted at 7 days post infection and proviral DNA levels were measured by alu-gag qPCR. Viral protein 24 (p24) levels in the culture supernatants were measured at day 12 using ELISA p24 antigen assay (Lenti-X p24 Rapid Titer Kit, TaKaRa). Briefly, culture supernatants were centrifuged and filtered through 0.45 μm filter to remove cell debris and diluted samples were run in duplicates. ELISA procedure was performed following the manufacturers protocol and plates were read on Magellan ELISA plate reader instrument (TECAN) at 450 nm.

Flow cytometry

Flow cytometric measurements were made on freshly isolated MC or MDM obtained by differentiation for 7 days in the presence of M-CSF. Prior to flow cytometry, adherent MDM were washed twice with Hank's balanced salt solution (HBSS) and released from the culture flask by treating with Accutase (Cell Technologies) for 30 min at 37˚C. MC and MDM were resuspended at a concentration of 10^6 cells/mL in $1 \times$ HBSS (pH 7.2), 5 mM EDTA and 0.5% BSA and passed through a 35 μm nylon mesh (BD Biosciences) before injection on a FACSCalibur flow cytometer (Becton Dickinson). For each cell type, 20,000 events were recorded for analysis. Dot plots were created using forward scatter (FSC-H) and side scatter (SSC-H) measurements to determine the size and granularity differences. All data were analyzed using Cell Quest software.

Light microscopy

MC were prepared as described above using the Pan-Monocyte isolation kit from Miltenyi. The obtained MC were resuspended in fresh RPMI medium and allowed to adhere on a glass

slide for an hour before collecting images at 20x magnification. MDM were differentiated from MCs as described above using RPMI media containing 10% autologous sera and M-CSF. After seven days, the adherent cells were visualized using 20x magnification and images were collected. Images were converted to 8-bit grayscale using ImageJ software.

Statistics

The data uncertainties are expressed as the mean ± 1 SD. Unless otherwise indicated in the figure legends, data are derived from at least three independent experiments using cells isolated from at least three donors. Experiments using cells from individual donors were performed in triplicate. Data were analyzed using the Prism 8.0 statistical program from GraphPad Software. Assessment for normality of the data was ascertained using the Kologorov-Smirnov test. For data sets that were not normally distributed, we tested the significance using a non-parametric Wilcoxon rank-sum test for unpaired groups. The cellular measurements were performed using three donor samples, and therefore, the Wilcoxon rank-sum test was also used for significance testing. To determine the statistical significance between mutational frequencies we used Fisher's exact test.

Results

dUTP/TTP in MDM and MC is high but variable with blood donors

In previous studies dUTP/dTTP ratios in the range 20:1 to 60:1 were reported [4,12,24], while the ratio was essentially zero in dividing cells due to the expression of dUTPase in replicating cells [4]. These different estimates of intracellular dUTP/dTTP may arise from the combined challenges of measuring low levels of dNTPs present in non-dividing cells, the inherent difficulty in accurately determining the ratio when one of the nucleotides is present at an extremely low level, intrinsic differences in dNTP pools in different donors, or differences in culture conditions or measurement methods.

We first extended the dTTP and dUTP measurements to freshly isolated monocytes with the expectation that the levels in freshly isolated cells would most closely match *in vivo* levels. A single nucleotide polymerase extension (SNE) assay was used where a 22 mer DNA primer-template containing a single adenine overhang on the template strand was extended by the dUTP or dTTP present in cell extracts (**Fig 1A**) [3]. The assay takes advantage of the enzyme dUTPase to remove dUTP in the extract and allow measurement of dTTP in isolation (see methods). Thus, the ratio of the intensities of the SNE extension bands to the original primer band gives the fractional extension arising from the sum [dTTP + dUTP]. When dUTPase is added before the reaction, the extension can only arise from dTTP and the level of dUTP-associated extension is determined by the difference in the fractional extension between the +/- dUTPase reactions. For these assessments, the [dTTP + dUTP] present in MC and MDM extracts were compared with the Hap1 dividing cell line (**Fig 1B** and **S1 Fig**). We found similarly low levels of [dTTP + dUTP] in freshly isolated MC extracts as compared to MDM that had been differentiated over seven days in the presence of M-CSF (1.1 to 2.5 pmol dU(T)TP/ million cells). For comparison, the combined [dTTP + dUTP] level in the Hap1 cell line is 25 to 70-fold higher (~70 pmol dU(T)TP/million cells). Depleting dUTP in these dNTP extracts by the addition of dUTPase allowed calculation of dUTP/dTTP in each cell type (**Fig 1C**). Although freshly isolated MC and differentiated MDM showed similar elevated dUTP/dTTP ratios in the range 1:4 to 1:1 depending on the donor, the ratio was essentially zero for the Hap1 cells. Based on these and previous studies, we conclude that significantly elevated dUTP/dTTP is an intrinsic aspect of MC and MDM metabolism that differs from dividing cells.

Although a range of dUTP/dTTP values have been reported for MDM [4,24], all of the measurements are consistent with low dNTP pools and significant levels of dUTP for both MC
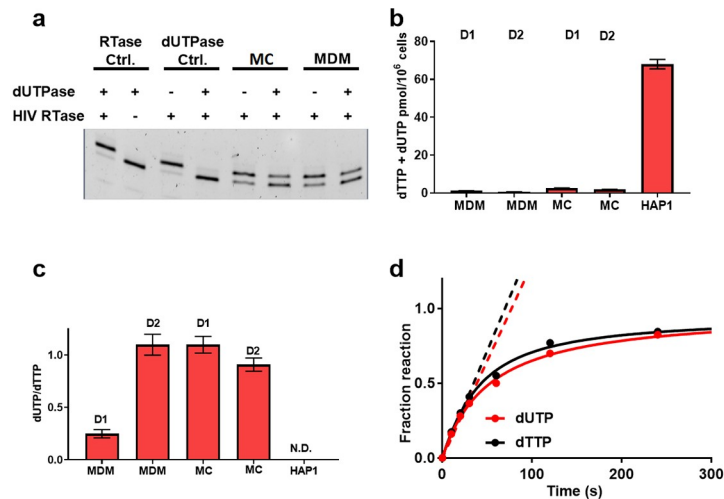
Fig 1. dUTP and dTTP pool measurements from methanol extracts of MDM, MC and comparison with Hap1 dividing cells. A single nucleotide extension assay (SNE) was used to measure dUTP and dTTP levels in MDM, MC and the Hap1 dividing cell line (S1 Fig). The specific measurement of dUTP in a mixed pool of TTP + dUTP is accomplished by the *in vitro* conversion of dUTP to dUMP + PP$_i$ using dUTPase prior to the SNE assay. (a) dUTP and dTTP pool measurements from methanol extracts of MDM, MC and comparison with Hap1 dividing cells. The RTase control (dTTP only) establishes that RTase is required for converting the *n* bp substrate into *n + 1* and that dUTPase does not inhibit extension in the absence of dUTP (see methods). The dUTPase control establishes that RTase can fully extend the probe by a single nucleotide in the presence of a dNTP mixture with dUTP replacing dTTP. The addition of dUTPase completely abolishes extension under these conditions. The ratio of the intensities of the SNE extension bands to the original primer band gives the fractional extension arising from [dTTP + dUTP] ie. (n+1 band)/{(n + 1 band) + (primer band)}. When dUTPase is added before the reaction, the extension can only arise from dTTP. Thus, the level of dUTP associated extension is determined by the difference in extension between the +/- dUTPase reactions. (b) Combined dTTP + dUTP pool measurements for MDM and MC from two donors (D1 and D2) and the Hap1 dividing cell line. Error bars are standard errors from triplicate measurements. (c) dUTP/dTTP ratio for the various cell types. ND, not detected. Error bars are standard errors from triplicate measurements. (d) Determination of the relative activity of HIV RTase for incorporation of dTTP or dUTP opposite to adenine. The solid line is a theoretical fit to the entire time course, while the dashed lines are initial rate linear fits, which are statistically indistinguishable. The concentration of the template DNA was 50 nM and concentration of each dNTP was 100 nM, which is the estimated concentration of these dNTPs in MDM or MC.

and MDM. The current measurements indicate that uracilated viral cDNA will be produced during infection of both MC and MDM and that the UBER capacity of these cells could impact the outcome of infection. However, unlike previous studies where dUTP/dTTP > 20, the more or less balanced ratio (~1) indicates that viral dUMP residues have the potential for being replaced by dTMP after multiple repair cycles (i.e. each replacement attempt has a 50:50 chance of replacing dUMP with dTMP, but eventually all dUMP would be repaired).

To evaluate whether HIV RTase can discriminate between dUTP and dTTP, and therefore bias dUMP incorporation away from the level expected from the dUTP/dTTP ratio, we measured the RTase activity *in vitro* using both dUTP and dTTP as substrates (**Fig 1D**). Using a low dNTP concentration that approximated that calculated for non-dividing cells, we were unable to detect any selectivity of RTase for either nucleotide. Thus, the relative amounts of dUMP and dTMP in HIV reverse transcripts should reflect the cellular dUTP/dTTP.

## MC and MDM have different Uracil Base Excision Repair (UBER) activities

Given that RTase shows no discrimination between dUTP and dTTP, the observed ratios of dUTP/dTTP of 0.25 to 1 for MDM and MC indicate that 99.9% of HIV DNA products would have at least one dUMP incorporation for every turn of the DNA helix assuming a random

sequence containing 50% A/T base pairs. These putative densely spaced uracils would be subject to excision by the UBER pathway. Accordingly, we were interested in the relative levels of six enzymes involved in deoxyuridine metabolism in MC and MDM as compared to the Hap1 dividing cell line (**Fig 2**). These enzymes included uracil DNA glycosylase (hUNG), AP endonuclease 1 (APE1), DNA polymerase β (pol β), ligase IIIα (the ligase isoform expressed in nondividing cells) [25], and the DNA cytidine deaminases APOBEC3A (A3A) and APOBEC3G (A3G). The western blots and activity measurements for extracts collected from uninfected cells and MC and MDM that were infected with the CCR5 tropic HIV-1^{BaL} viral strain revealed the following general trends (**Fig 2A–2J**). First, MC and MDM show similarly low levels of expression of the first enzyme in the UBER pathway (hUNG), which are about 25 to 50-fold lower than the Hap1 reference line. These low hUNG activity levels, which could result from either the mitochondrial (hUNG1) or nuclear isoforms (UNG2), indicate that viral uracils may not be efficiently excised once viral DNA enters the nuclear compartment. Surprisingly, the activity of the next UBER enzyme, APE1, is highly expressed in both MDM and Hap1 cells, indicating that the rate-limiting step for repair of uracil in non-dividing cells is likely the initial excision event by hUNG2. Its high expression level is consistent with previous activity measurements of APE1 in MDM and MC extracts and it is unlikely to be rate determining in any uracil repair that may be occurring (even with the modest reduction in its level upon Bal virus infection, see below). The next two enzymes in the pathway, pol β and lig IIIα, are almost undetectable in MC but much more prevalent in MDM, although not to the same level as the Hap1 line. This important distinction between MC and MDM suggests that uracilated viruses generated by direct infection of MC cannot be repaired until the MC differentiate into MDM. Both deaminase enzymes, A3G and A3A, are highly expressed in MC, but not MDM or Hap1 cells. Despite the high expression levels of A3G and A3A, the high dUMP content of viral DNA in MC is not derived from intrinsic A3A or A3G activity—at least not with HIV-1^{BaL} virus that encodes viral infectivity factor (*vif*) (see below). Except for APE1, which showed a ~2-fold decrease in its expression level upon Bal virus infection of MC (**Fig 2C**), none of the expression data were noticeably affected by whether the extracts were prepared before or after BaL virus infection. We performed additional quantitative RT-qPCR measurements of mRNA expression levels of these genes which were fully consistent with the above trends (**S2 Fig**).

HIV infection of MC and MDM at early and late stages of differentiation

To explore the origins and possible fate of infected circulating monocytes observed in HIV patients on ART, we performed HIV infections using freshly isolated, undifferentiated MC rather than fully differentiated MDM. We began this exploration by measuring the levels of dUMP present in proviral DNA under three distinct conditions (i) MC that were infected with HIV-1^{BaL} immediately after isolation and then maintained as undifferentiated monocytes for 7 days by culturing under nonadherent conditions in the absence of M-CSF, (ii) MDM infected at the monocyte stage and then allowed to differentiate in the presence of M-CSF (*Early Infec*tion, MDM^{EI}) and, (iii) MDM that were infected after seven days of differentiation in M-CSF (*Late I*nfection, MDM^{LI}) (**Fig 3A**). For comparison, we infected activated T cells using the same virus stock and MOI. Proviral dUMP levels were determined using the alu-gag Ex-qPCR experiment after isolating genomic DNA at 1, 3, 7, 14- and 28-days post infection (dpi). To prevent multiple round infection, 0.2 μM enfuvirtide (T-20) was added one day after the initial infection (**Fig 3A**). The Ex-qPCR analysis determines the fraction of integrated HIV viruses in a DNA sample that contain one or more dUMP residues on each DNA strand of a DNA amplicon that contains a 650 bp region of the 5' LTR and a 700 bp portion of the gag gene [4,26]. For MC, which were cultured using non-adherent conditions in the absence of M-CSF to
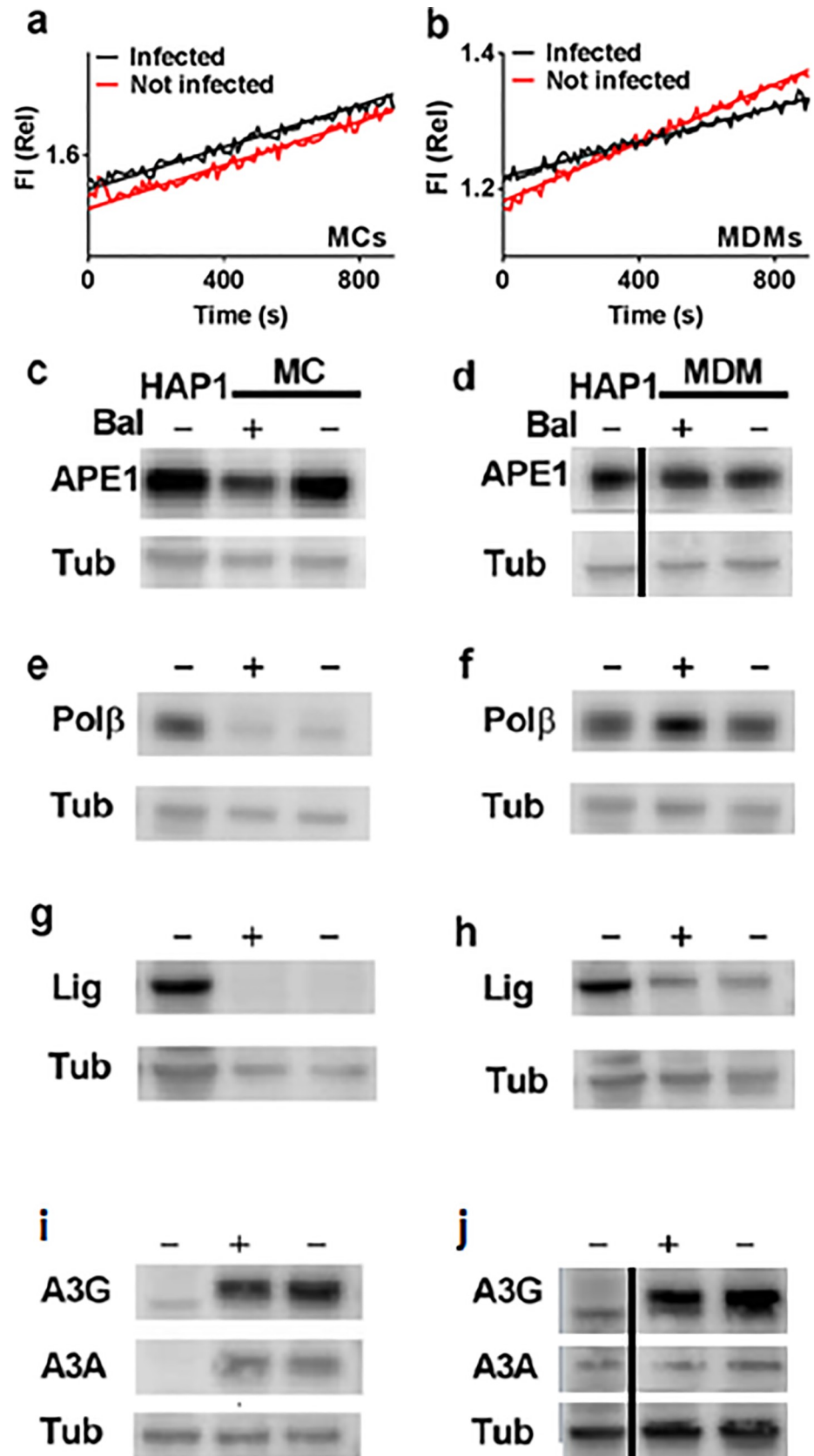
Fig 2. Determination of Uracil Base Excision Repair (UBER) capacity of infected and uninfected MCs, MDMs and comparison with the Hap1 dividing cell line. MC or MDM were infected with replication competent CCR5 tropic HIV-1^{BAL} virus at MOI = 5. Extracts from MC (a, c, e, g, i) and MDM (b, d, f, h, j) using uninfected (-) or infected cells (+) at 3 days post-infection were processed for western blotting. Blots were performed using 10 μg of total cell protein, except for Lig IIIα, where 20 μg was used. Due to the low levels of hUNG present in non-dividing cells, native extracts (10 μg) were prepared for measurement of UNG enzymatic activity using a sensitive real-time fluorescence assay (see methods). The specific measurement of UNG activity was established by the addition of UNG inhibitor UGI (4 μM), which completely inhibited the measured activity. Panels a to j show western blots or activity assays for detection of (a, b) uracil DNA glycosylase (UNG); (c, d) AP endonuclease 1, (APE1); (e, f) DNA polymerase β, (polβ); (g, h) ligase III (Lig); and (i, j). APOBECA3A (A3A) and APOBECA3G (A3G); tubulin (Tub) loading control was used in each blot.

maintain a monocyte-like phenotype (S3 Fig), no proviral DNA was detected at 1 dpi, but by day three nearly 100% of the proviral copies contained dUMP, which persisted until the end of the experiment (7 dpi)(Fig 3B). Due to limitations in the length of time MC can be maintained using nonadherent conditions, this experiment could not be continued beyond seven days. For MDM^{EI}, which were infected immediately after isolation of MC and then cultured using adherent conditions in the presence of M-CSF to immediately begin their differentiation into MDM, over 50% of the provirus contained dUMP at 1 dpi, which increased to almost 100% at 3 dpi. Unlike MC grown under non-adherent conditions in the absence of M-CSF, the copies of HIV in MDM^{EI} that contained dUMP decreased by 7 dpi (Frac U ~ 75%) and even further at 14 dpi (Frac U ~ 20%). For MDM^{LI}, which were infected after complete differentiation, the proviral copies that contained dUMP were initially lower than MC or MDM^{EI} (Frac U ~ 15% at 1 dpi and 60% at 7 dpi), but ended up at the same level as MDM^{EI} at 14 dpi (Frac U ~ 20%). We attribute the lower Frac U values of differentiated MDM at early times after infection to the greater rate of reverse transcription in a small sub-population of permissive MDM (<10%) which have higher dNTP pools and low dUTP [4]. As the post-infection time increases, the slower replicating uracilated DNA products in the major MDM population increasingly contributes to the bulk measurement. The control T cells showed no viral-associated dUMP at any time during infection, consistent with our previous finding (4).

We then investigated the kinetics for appearance of early and late reverse transcripts (ERT, LRT) and proviral DNA using the three infection conditions. The kinetics for forming ERT and LRT products followed the trend MDM^{LI} > MDM^{EI} >> MC (Fig 3C and 3D), with ERT and LRT copy numbers for MDM^{EI} and MC about 2 and 6-fold lower at 7 dpi as compared to MDM^{LI}. A similar trend was observed for the proviral copy numbers (Fig 3E). The control infections of activated T cells showed both faster reverse transcription kinetics (~70% complete in ~1 day, Fig 3C, 3D and 3E) and a greater number of integrated proviruses.

dUMP in proviral DNA does not arise from cytidine deaminase activity in MC

Given the presence of APOBEC enzymes in MC, and to a lesser extent MDM as judged by immunoblotting (Fig 2I and 2J), we wanted to confirm that most of the dUMP in HIV proviral DNA was derived from incorporation of dUMP by RTase. One established way to test this is to add high levels of thymidine (dThyd) to the cell culture media prior to infection to increase the levels of intracellular TTP and then look for a reduction in the number of viral DNA products that contain dUMP [4]. We infected both MC and fully differentiated MDM in the presence of 5 mM dThyd and measured the copies of uracilated proviruses at 7 dpi using the Alu-gag Ex-qPCR method (Fig 4). For both cell types we observed a 4-8-fold reduction in uracilated viral copies, indicating a predominant role for dUMP incorporation. A further reduction in uracilated viral copies is not expected due to the minor population of highly
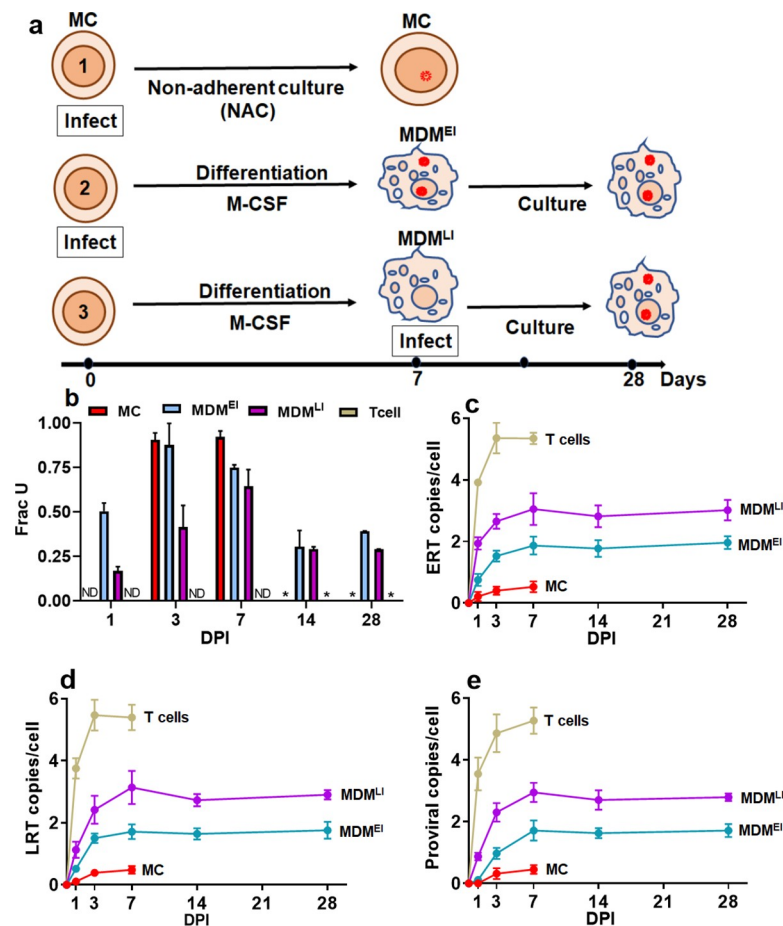
Fig 3. Characteristics of HIV infection in MC and macrophages infected before differentiation (MDM^{EI}) and after differentiation (MDM^{LI}). (a) Infection of MC and MDM with HIV-1^{BaL} virus was performed using three conditions (MOI = 5). In one condition, MC were immediately infected and then cultured using nonadherent conditions without M-CSF for seven days to maintain a monocyte phenotype. MDM^{EI} refers to "early infection" of freshly isolated MC, which were subsequently differentiated into MDM under adherent conditions in the presence of M-CSF. MDM^{LI} refers to "late infection" where MDM were first fully differentiated before infection. In all cases, HIV fusion inhibitor drug, enfuvirtide, (0.2 μM final concentration) was added to culture medium after 24 hours of infection to prevent multiple rounds of infection. (b) Fraction of provirus in MC, MDM^{EI} and MDM^{LI} that contain uracil as determined by alu-gag Ex-qPCR. ND: not detected (c) Time course for appearance of early reverse transcription (ERT) products as determined by RT-qPCR using a primer set targeting the 5'LTR region of the HIV genome. (d) Time course for appearance of late reverse transcription (LRT) products as determined by RT-qPCR using a primer set targeting the LTR region of the HIV genome. (e) Time course for appearance of proviral DNA copies determined by alu-gag qPCR. Identical infections activated T cells were used as controls and are shown in panels d, e and f. Abbrev: ND, not detected. * not done. All data are averages obtained from three blood donors.

permissive MDM that do not contain high dUTP levels [4,27]. A minor role for APOBEC DNA cytidine deamination is confirmed by our proviral DNA sequencing results reported below, which show a low frequency of G to A transition mutations on the proviral (+) strand DNA at known APOBEC hotspots.

Effect of viral dUMP on proviral DNA and extracellular RNA sequences

To investigate proviral DNA sequences produced by reverse transcription in both MC and fully differentiated MDM, we used HIV-1^{BaL} virus to infect freshly isolated MC cultured under non-adherent conditions and also MDM after 7 days of culturing. Both cell types were
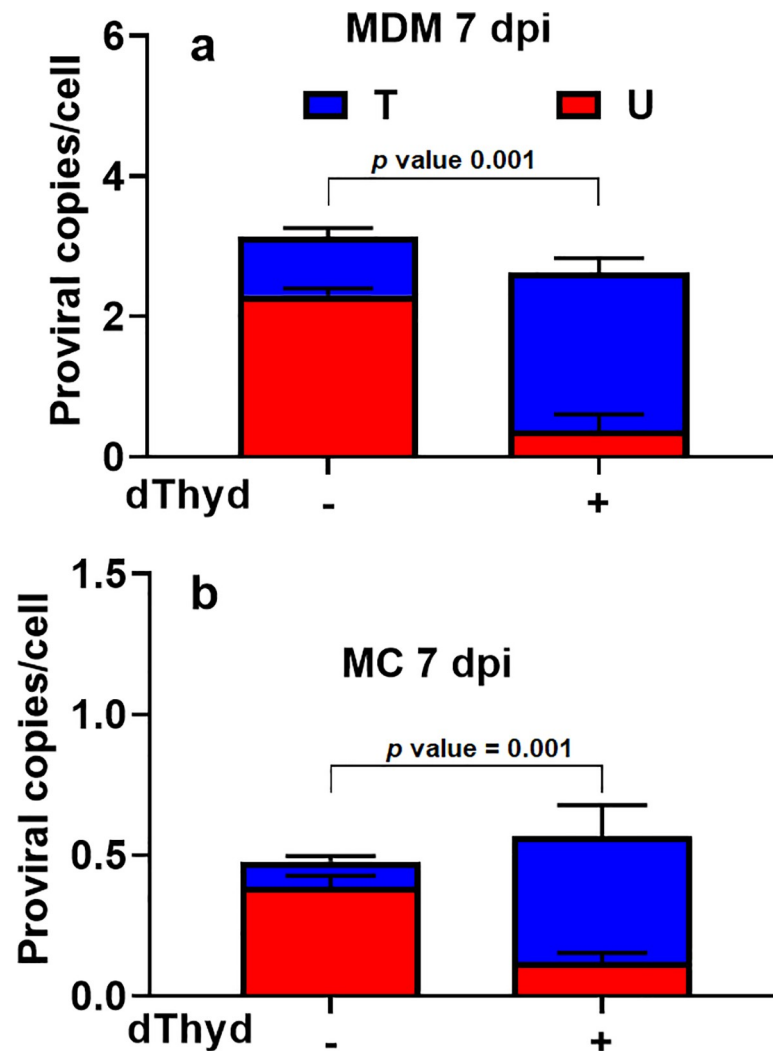
Fig 4. dUMP in HIV DNA during infection of MC and MDM arises predominantly from dUTP. MC and MDM[LI] were infected with HIV-1[Bal] virus at an MOI of 5 (1 pg p24/cell) in the presence (+) and absence (-) of 5 mM deoxythymidine (dThyd). Copy number measurements of uracilated (red) and non-uracilated (blue) proviruses were made 7 dpi using the Alu-gag Ex-qPCR method. (a) MDM[LI] and (b) MC infected in the absence and presence of dThyd. *p*-values from an unpaired Student's *t*-test are shown.

cultured for seven days after infection and total DNA was isolated and diluted to the single copy level. Single proviral clones were then amplified using ES7 and ES8 env primers (see **S1 Table**). Wells that were positive for HIV DNA clones by qPCR were reamplified using primers that generated a 592 bp amplicon covering the V3 and V4 regions of *env*, followed by sequencing using the Sanger method. The viral sequences were compared with the lab reference sequence to determine the mutation frequencies and types. For proviral sequences isolated from MC and MDM, the viral mutation frequency (~1.4 x 10^{-3}) and mutational spectrum were similar (**Table 1, Fig 5A and 5B**). For both cell types, 26 to 38% of the isolated proviral clones contained substitution mutations, with the majority appearing as transition mutations (~70–80%), and the remaining being more unusual transversion mutations (20% to 30%). Two (+) strand G→A mutations detected in both MDM and MC infections might be attributed to enzymatic cytosine deamination on the viral (-) strand cDNA based on the sequence

Table 1. Mutational analysis of HIV proviral DNA and extra cellular viral RNA extracted from infected MC and MDM[a].

Cells	DNA treatment	Total Clones	bp Sequenced	Mutated Clones	Point Mutations	Mutation Freq.	Transitions	Transversions
MC	None	16	8554	6 (38%)	11	1.3×10^{-3}	9 (82%)	2 (18%)
MDM	None	35	18165	11 (26%)	26	1.4×10^{-3}	19 (73%)	7 (27%)
MDM	dUMP depleted[b]	44	21956	15 (34%)	19	0.86×10^{-3}	16 (94%)	1 (6%)
MDM (gRNA)	None	20	10280	13 (65%)	17	1.7×10^{-3}	13 (76%)	4 (24%)

[a]MDM were infected as described in Fig 4 and the nucleic acid was isolated at 6 dpi and processed for LD-sequencing. Mutation frequencies are calculated based on total bases sequenced i.e. frequency = mutated bases/total bases sequenced).

[b]This DNA sample was depleted in the copies that contained dUMP by *in vitro* digestion with UNG prior to LD-sequencing.

https://doi.org/10.1371/journal.pone.0235012.t001

preferences of A3A or A3G (S2 Table). However, for MDM we cannot exclude that these apparent enzyme derived mutations arose from chance misincorporation because four G→A mutations occurred on the viral (-) strand cDNA (corresponding to C→T on the positive strand). These mutations in MDM cannot be attributed to APOBEC activity because of their sequence context and occurrence on the (-) strand (S2 Table). The two (+) strand G→A mutations observed in the MC derived samples could arise from the high A3A activity in these cells. Finally, 40% and 55% of the proviral mutations in MDM and MC led to codon changes and could therefore affect viral fitness (S2 and S3 Tables).

We also sequenced extracellular viral RNA produced from HIV-1[BaL]-infected MDM[LI]. The viral RNA sequences showed a slightly elevated mutation frequency compared the proviral DNA (1.7×10^{-3}) and similar percentages of transition and transversion mutations. In addition, about 65% of the viral RNA mutations led to codon changes, including two stop codons, two charge reversals, and several other nonconservative amino acid changes (S5 Table). Although some of these mutations are present in HIV sequence databases, there is no available information on their functional impact.

Selective sequencing of dUMP-depleted DNA fraction

We were interested in whether a different mutational spectrum might result if the fraction of proviral DNA that contained dUMP was subtracted from the total population of proviral DNA before single-molecule amplification and sequencing. To address this question, we performed UNG digestion on the total DNA extracted from infected MDM to remove all of the dUMP-containing copies prior to PCR amplification and then repeated the limiting dilution steps and clonal sequencing (Fig 5B). Although the dUMP-depleted DNA showed a modest 2-fold reduction in the mutation frequency (0.8×10^{-3}) (Table 1, S4 Table), this reduction was not significant (*p*-value = 0.16). Despite the insignificant effects on the mutation frequency, the mutation spectrum for the dUMP-subtracted DNA fraction consisted almost entirely of transition mutations, with only a single transversion mutation after sequencing 21,958 bases (Fig 5B). Thus, transversion mutations appear to be correlated with the DNA fraction that contains dUMP.

To explore why DNA clones containing dUMP showed a higher frequency of transversion mutations, we examined the average [A + T(U)] content for 7 mer sequences centered on these transversion sites to explore whether the mutations might be correlated with the density of dUMP incorporation on either the (+) or (-) strand. For comparison, we determined the average [A + T(U)] content of the 7 mer sequences surrounding the transition mutation sites in the dUMP-depleted and total DNA samples (S2 and S4 Tables). This comparison showed a statistically higher average frequency of [A + T(U)] near the transversion sites ($\mu = 0.80$) as compared to the transition mutation sites (dUMP-depleted DNA, $\mu = 0.58$; total DNA, $\mu =$
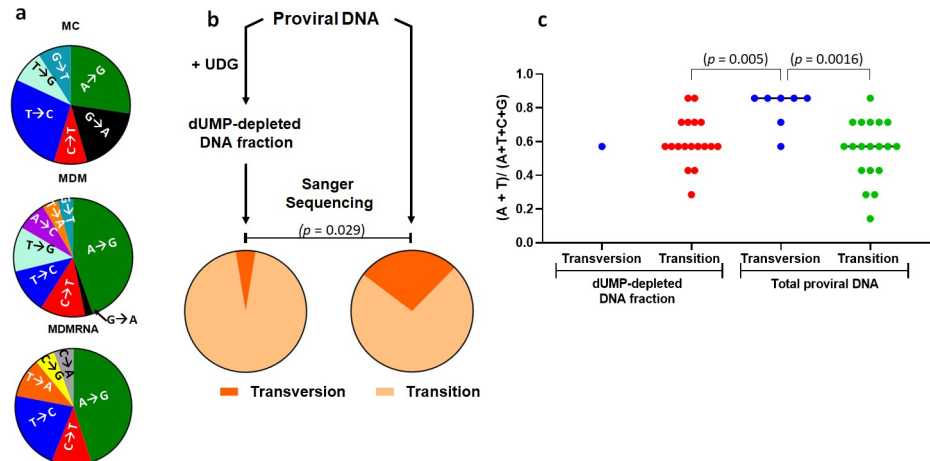
Fig 5. Mutagenic effects of uracil incorporation on HIV proviral DNA and extracellular viral RNA in MDM and MC. Sequences of single proviral clones and extracellular viral RNA from infected MDM and MC. MC and MDMs were infected with equivalent amount of virus (1 pg p24/cell). Seven days after infection total cellular DNA and extracellular viral RNA were extracted from cells and the culture supernatants, respectively. Single viral copies were amplified by limiting-dilution nested PCR and sequenced by the Sanger method. Sequences were aligned to our laboratory reference HIV-1^{BaL} sequence. (a) Mutational spectrum of HIV proviral DNA sequences from infected MC (left top), MDM (left middle) and extracellular viral RNA extracted from MDM (left bottom). (b) A population of viral cDNAs was sequenced before and after the removal of dUMP-containing sequences as indicated. Removal of dUMP-containing viral sequences was accomplished by treatment of the total DNA population with UNG prior to PCR amplification and clonal sequencing. HIV proviral DNA sequences where the dUMP fraction was subtracted contained almost exclusively transition mutations (left pie chart), while the total proviral DNA without subtraction showed the same transition mutations but also unique transversion mutations (right pie chart). (c) Transversion mutations are associated with loci that contain higher average A/T(U) content. In this analysis, the average A + T(U) content over a window of three flanking bases on both sides of each transversion or transition mutation was calculated. The loci with transversion mutations had a higher average content than the 29 loci that showed transition mutations. p-values from Wilcoxon rank-sum test indicate the statistical significance of the average A + T(U) content in the six base window surrounding the transition and transversion sites.

0.55) (**Fig 5C**). Using a chi square or Fisher exact test, the differences in the mean values were determined to be significant (p values < 0.03). Possible mechanistic implications of this result are discussed below.

Normalized viral output of HIV-1^{BaL} produced from MC, MDM^{EI} and MDM^{LI}

We determined the relative efficiency that MC, MDM and activated T cells produce virus particles and extracellular vRNA by normalizing the viral output by the average number of proviruses present in each infected cell type (**Fig 6**). Using p24 or extracellular viral RNA levels as the measure for output, there were only modest differences for the three myeloid cell infections at 7 dpi, although MDM that were infected after complete differentiation (MDM^{LI}) showed a 2-fold greater yield than MC. For comparison, activated T cells infected under identical conditions showed a 5-fold higher viral output than MC (**Fig 6A and 6B**), indicating an intrinsically higher efficiency than any of the infected myeloid cells.

We then investigated the normalized viral output of HIV-1^{BaL} produced from infected MC, MDM^{EI}, MDM^{LI} and activated T cells by collecting culture supernatants at 7 dpi and using equivalent copies of virus to infect MOLT-4/CCR5 target cells (**Fig 6C**). Seven days after infection of the target cells, total cellular DNA was extracted, and LRT copies were quantified using qPCR (**Fig 6D**) and p24 levels were measured in the culture media (**Fig 6E**). Although equal p24 units were used in each of the infections, the target cell LRT copies were about 4-fold greater for infections initiated with viral supernatants obtained from MDM^{LI} as compared to
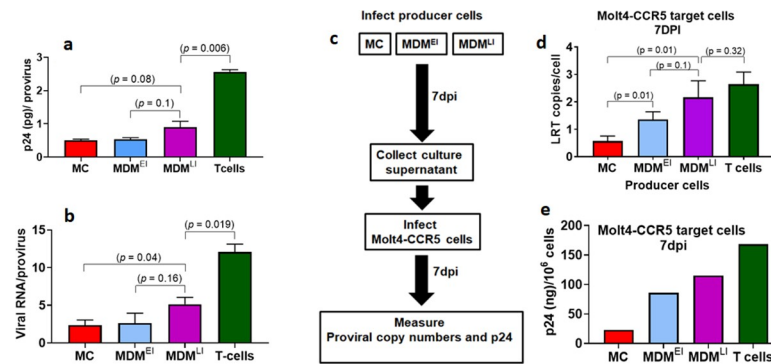
Fig 6. Normalized viral output from HIV proviruses in MC, MDM and activated T cells. All cell types were infected with Bal virus at MOI of 5 (1 pg p24/cell) and seven days after infection culture supernatants and cellular DNA were processed. MC were infected immediately after isolation and then cultured for seven days without differentiation using nonadherent conditions in the absence of M-CSF. MDM^{EI} were infected as freshly isolated MC and then differentiated into MDM under adherent conditions in the presence of M-CSF. MDM^{LI} were infected after differentiation for seven days in the presence of M-CSF. T cell controls were infected and cultured in IL-2 medium for seven days. T20 entry inhibitor (10 μM) was used to prevent reinfection. (a) Viral protein 24 (p24) levels in culture supernatants were measured by ELISA and normalized to total proviral copies determined by alu-gag qPCR. (b) Extracellular viral RNA was measured using RT-PCR and normalized to total proviral copies determined by alu-gag qPCR. p-values from an unpaired Student's t-test are shown. (c) Experimental scheme for determining infectivity of virus generated from MC, MDM^{EI} and MDM^{LI} producer cells. (d) Viral supernatants from MC, MDM^{EI} and MDM^{LI} and T cell producer cell cultures were collected at 7 dpi and MOLT-4/CCR5 target cells were infected using a 0.1 pg p24/target cell. Seven days after infection of target cells, cellular DNA was extracted and levels of proviral DNA were determined by qPCR. Relative infectivity is shown as LRT copies per target cell. p-values from an unpaired Student's t-test are shown. (e) p24 levels were measured by the ELISA method. The data were obtained from one of the three donor samples analyzed at the proviral level in panel d.

MC, while MDM^{EI} showed an intermediate level of LRT copies. In addition, supernatant p24 levels were 6-fold greater for infections initiated with MDM^{LI}. These differences indicate that the fitness of viral particles produced from MC is lower than MDM despite the similar efficiency of production from integrated viruses. If we define an infection cycle that begins with viral infection of a MC or MDM and ends with the infection of a new target cell, we calculate an overall 50-fold lower normalized viral output from MC as compared to a fully differentiated MDM. This comparison between the two cell types is based on the product of the relative efficiencies for virus integration (**Fig 3**), viral particle production from integrated virus (**Fig 6A and 6B**) and the productive infection of new target cells (**Fig 6D and 6E**). Using the same calculation, MC have normalized viral output that is 300-fold less than activated T cells. It is not clear at this time how much viral dUMP levels or UBER contributes to the lower normalized output in myeloid cells.

Expression of exogenous hUNG2 before HIV infection depletes uracilated HIV DNA products

Because of the low expression level UBER pathway enzymes detected in MDMs, and especially the very low hUNG2 activity observed in both monocytes and MDMs (**Fig 2A and 2B**), we hypothesized that low hUNG2 levels might limit the restrictive effects of the UBER pathway. To test this hypothesis, we over-expressed full-length human UNG (hUNG2) in MDMs using a doxycycline inducible lentiviral transduction system. The inducible system allowed us to test whether hUNG2 expression had a greater effect before HIV infection, or alternatively, after HIV had integrated into the MDM genomic DNA. Control experiments demonstrated the presence of high hUNG2 activity in cell extracts prepared from transduced MDM at days 1 and 3 post induction, but no activity in the absence of doxycycline induction (**S5 Fig**).
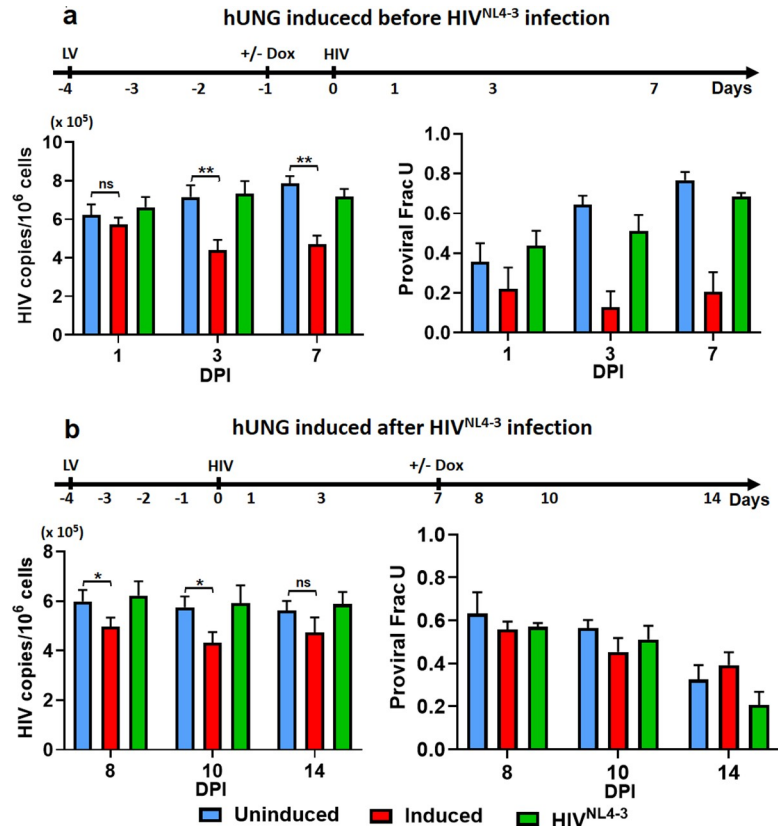
Fig 7. Exogenous expression of hUNG2 depletes uracilated HIV DNA products. Exogenous full-length hUNG2 was over expressed in MDM under control of a doxycycline (Dox) inducible promoter by lentiviral transduction (MOI = 5). The timelines above each panel indicate the experimental course and the points where hUNG2 expression was induced relative to infection with HIV^{NL4-3}. (a) hUNG2 expression was induced with doxycycline (1 μg/ml) one day before HIV^{NL4-3} infection. Proviral copy numbers (left panel) and the fraction of HIV proviral DNA that contained dUMP were measured at indicated times (FracU, right panel). (b) Expression of hUNG2 was induced 7-days after infection with HIV^{NL4-3} in order to allow HIV to fully integrate. Proviral copy numbers (left panel) and the fraction of HIV proviral DNA that contained dUMP were measured at indicated times (FracU, right panel). Uninduced (blue) and no lentiviral infection (green) controls were also performed.

https://doi.org/10.1371/journal.pone.0235012.g007

We first tested the effect of inducing hUNG2 expression prior to infection with VSVG pseudo-typed HIV^{pNL4-3} virus particles capable of only a single round infection. In this experiment, fully differentiated MDM were first transduced with the hUNG2 expressing lentivirus at an MOI of 5 (0.1 pg p24 antigen/cell) and expression of hUNG was induced using 1μg/ml of doxycycline three days after transduction, followed by infection with HIV^{NL4-3} one day later (MOI = 0.5) (**Fig 7A**). We followed the HIV provirus copy number and the fraction of total provirus that contained dUMP using alu-gag Ex-qPCR. These measured outcomes were compared with those of an uninduced control infection (blue bars, **Fig 7A**), as well as an infection with HIV^{pNL4-3} in the absence of any prior lentiviral transduction (green bars, **Fig 7A**). With pre-infection induction of hUNG2 expression (red bars, **Fig 7A**), there was a 50% decrease in the provirus copy number between 1- and 7-days post HIV^{pNL4-3} infection and the fraction of proviruses containing dUMP was at the limit of detection for the Ex-qPCR method (< 0.2). In contrast, the no induction and HIV^{NL4-3} only control infections showed a stable or slightly increasing proviral copy number over the same time period and the fraction of proviruses containing dUMP increased from ~0.4 to 0.8. Similar results were obtained using LRT primers for Ex-qPCR (**S6 Fig**). As discussed above and previously [4,27], the reduction in proviruses as a

result of UNG overexpression is never complete because the MDM exist as a mixed G1-G0 population where only about 40–50% of the total proviruses contain dUMP. In contrast, the essentially complete absence of viral dUMP at one to seven days post infection as measured by alu-gag Ex-qPCR clearly indicates cellular hUNG2 excised the uracils prior to viral integration. These results indicate that when hUNG2 is abundant in the target cell prior to HIV infection, uracilated viruses can be efficiently destroyed before integration.

In a second experimental protocol, hUNG2 induction was delayed until 7 days after HIV^{NL4-3} infection to allow most of the HIV cDNA to integrate (**Fig 7B**). Under this infection scenario we saw a smaller decrease in HIV proviral DNA between 8- and 14-days post-infection (one to seven days post-induction) as compared to the pre-infection induction of hUNG2 shown in **Fig 7A**. In addition, a higher fraction of proviruses contained dUMP and these proviruses slowly disappeared over one to seven days post-induction. In fact, the rate of decrease of dUMP-containing proviruses was not significantly different for the hUNG2-induced condition and the uninduced controls (**Fig 7B**). This indicates that the rate-limiting step for post-integration excision of uracils does not involve hUNG2 and may instead involve remodeling of chromatin.

Discussion

dUTP-mediated innate immunity was first suggested for β-retroviruses, non-primate lentiviruses, and endogenous retroviruses [28–31]. These viruses have all captured a host dUTPase gene during viral evolution, which is a powerful enzyme that degrades dUTP to dUMP and PP$_i$, promoting infection of macrophages by these viruses. Although HIV-1 does not encode for dUTPase, it can infect human monocytes and macrophages even though the ratio dUTP/TTP is large. One strategy that HIV uses to replicate in this environment is to code for the accessory protein vpr, which is used to target hUNG2 for ubiquitination and proteasomal degradation [16,32], suggesting that incorporation of dUTP is tolerated but that the antiviral function of hUNG2-catalyzed uracil excision must be overcome. Consistent with this phylogenetic comparison of different retroviruses, our previous work established that this dUTP-mediated restriction pathway works most potently when target cell dUTPase expression is low, dUTP is abundant, and nuclear hUNG2 is highly expressed so as to efficiently degrade viral cDNA [3,4]. When any of these elements are absent or diminished, the effectiveness of the restriction pathway is diminished, which likely explains diverse reports in the literature concerning the impact of this pathway [29,33–35]. Accordingly, quantification of cellular [dUTP]/[dTTP] and UBER enzyme expression levels are key to understanding the impact of this pathway in MC and MDM.

Implications of UBER activity and [dUTP]/[dTTP] in MC and MDM

Since MC differentiate into macrophages, it is possible that a macrophage originally infected at the MC stage of differentiation might produce different amounts and sequences of virus compared to a macrophage that was infected after complete differentiation. This question pertaining to the order of infection is relevant because MC containing uracilated viral DNA have been detected in blood samples of HIV patients on ART who are in full remission (10–600 infected MC/10^6 cells) [4,19]. This observation is intriguing because peripheral blood MC have a limited half-life of about 2 days in circulation and in this limited period infection must occur. After infection, MC either migrate to lymphoid tissues and differentiate into macrophages or are eliminated [20]. We speculate that under virally repressed conditions MC are most likely infected while passing through a tissue reservoir containing HIV infected cells and then enter back into circulation via retrograde migration before dissemination to other tissues [22,23].

Here we have demonstrated the kinetic competence of the MC infection pathway *in vitro* through the detection of viral cDNA products in MC within a relevant time frame (**Fig 3C–3E**). Since MC have high dUTP levels, but the entire UBER pathway is almost absent with the exception of APE1 (**Fig 2**), dUMP-containing proviruses likely persist throughout the MC lifetime. Thus, infected MC harboring uracilated viral DNA may successfully migrate to a tissue compartment and differentiate into macrophages. Once differentiated into macrophages, UBER activity is upregulated and dUMP can be slowly excised and at least partially replaced with dTMP. This mechanism is supported by the time-dependent decrease in viral dUMP over 28 days in MDM (**Fig 3B**), with no change in proviral copy number, suggesting that dUMP is being replaced by dTMP via UBER. This mechanism requires that the dTTP concentration is competitive with dUTP to prevent futile cycling (futile cycling is the excision of dUMP and its reincorporation by DNA pol). The measured [dUTP]/[dTTP] ~1 in macrophages in our *in vitro* culture conditions is compatible with a repair mechanism that allows slow nucleotide replacement over time (**Fig 1**). In contrast, the [dUTP]/[dTTP] in the range 20 to 60 as found in two previous studies would effectively prevent repair, and excision of such densely spaced uracils by hUNG2 would likely lead to fragmentase of the viral DNA as previously indicated [3,4,24]. If the [dUTP]/[dTTP] ratio is variable *in vivo*, it will have an impact on the efficiency of HIV infection of myeloid lineage cells, with outcomes ranging from slow repair to viral destruction depending on the dUMP density and hUNG2 expression levels.

UBER may occur after switching of macrophages from a G_0 to G_1 cell cycle state

Mlcochova *et al* reported that non-dividing MDM exist in two interconvertible cell cycle populations, a minor population that exhibits markers of G_1 and is DNA repair competent and a predominant population that is G_0-like and deficient in the expression of many DNA repair proteins and DNA replication components [27]. The two states can also be detected by infection with an HIV construct containing an eGFP expression cassette [4,27,36]. In this case, the restrictive G_0 population shows little or no eGFP fluorescence, even though viral cDNA is present in nearly every cell, while the permissive G1 population shows high eGFP expression [4,36]. These observations of Mlcochova *et al* parallel our previous measurements using a fluorescent reporter virus [4]. In our previous study we sorted infected MDM into GFP positive and negative populations and found that the GFP positive (G_1) population did not contain any detectable dUTP and the viral DNA was free of dUMP (4). In contrast, the GFP-negative (G_0) population contained high [dUTP] and the viral DNA also contained high levels of dUMP [4]. More recent work on the effects of dUMP on transcription of DNA templates by RNA pol II establishes that the differences in GFP expression between the two populations is at least partly due to transcriptional repression by dUMP [9]. Thus, these combined findings suggest that UBER may occur after an infected G_0 macrophage transiently moves to the G_1 state where the nucleotide pool composition and DNA repair capacity can facilitate dUMP removal and replacement. We speculate that small molecules that target the G_0-G_1 checkpoint might be useful to induce the transition to the G_1 state and potentially lead to inactivation of heavily uracilated proviruses by upregulation of UBER.

The realization that bulk MDM consist of two cell populations with respect to dUTP levels and UBER capacity further informs our understanding of the observation that only a fraction of total viral cDNA molecules contain dUMP. For instance, assuming a homogenous MDM population, it is difficult to rationalize why only ~60% of total proviruses contain dUMP within a 1200 base pair amplicon (**Fig 3B**). This fraction is enigmatic because with [dUTP]/[dTTP] ~ 1 and the inability of reverse transcriptase to discriminate between dTTP and dUTP

(**Fig 1**), every 10 bp of viral DNA should contain dUMP on both strands and all proviruses should contain dUMP. Thus, the low fraction of uracilated proviruses in MDM is consistent with the presence of two cell sub-populations and only one of the populations (G_0) contains high [dUTP]/[TTP]. In contrast, the observation that nearly all copies of HIV contain persistent dUMP during infection of MC suggests that the G_1 population does not exist to a significant extent before differentiation into MDM. Consistent with this model, MC show virtually no eGFP expression upon infection with a GFP reporter virus even though proviral DNA is present in nearly every cell (**S4 Fig**).

Potential mechanisms for mutational effects of dUTP incorporation by reverse transcriptase

There are surprisingly few studies of the mutational events during HIV infection of MDM, and to our knowledge, no previous reports of HIV sequences derived from infection of MC. The most complete and direct comparison of HIV mutations arising during single round infection of T cells and MDM is the next-generation sequencing study of full-length HIV genomes by Cromer et al [37]. In this study, the reported overall mutation frequency was ~1 x 10^{-4} for both cell types. Their reported HIV mutation spectrum for MDM infections (G→A = 35%, A→G = 18%, A→T = 17%, A→C = 11%) does not differ significantly from the profile obtained in our selective sequencing of a 500 bp amplicon covering the V3 and V4 regions of *env*, which is known to be highly variable (**Fig 5B**) [38,39]. However, our mutation frequency for this select region (1.4 x 10^{-3}, **Table 1**) is significantly higher than the average value previously reported by Cromer et al for the entire HIV sequence. This result is not unanticipated because we have previously reported that the mutation frequency for HIV DNA and RNA isolated from infected MDM is variable across the HIV genome [4]. In particular, the LTR region has very low levels of mutations [4].

One significant observation in our sequencing studies was that transversion mutations in proviral DNA were not detected in DNA samples where the dUMP fraction was subtracted by UNG digestion (**Table 1**, **Fig 5C**). This result indicates that the mutational profile for misincorporation of nucleotides by reverse transcriptase is indirectly impacted by the presence of dUMP in the (-) or (+) strand sequences. Although the detailed mechanistic basis for this outcome is not known, the sites of these transversion mutations are especially AT(U) rich (**Fig 6B**), suggesting that uracils on either strand may be involved (**S2 Table**). There is currently no information about the stability or dynamics of dUMP base pairs in the context of RNA/DNA hybrids, the possible sequence contexts that might give rise to mutational hotspots, or the activity of reverse transcriptase under such conditions. Relevant to the current findings, previous work on dUMP/A base pairs in duplex DNA has shown increased base pair dynamics and decreased thermodynamic stability [40,41,42]. The increased dynamics has been studied using NMR imino proton exchange and attributed to the reduced electron density of the base, which leads to poorer stacking interactions with neighboring bases [41]. Such effects in the context of RNA/DNA hybrids containing densely spaced dUMP substitutions are anticipated but require detailed biochemical studies to confirm. In this regard, we recently reported reduced fidelity of T7 RNA polymerase during transcription of RNA using a DNA template that contained dUMP [9]. These mutations were also explained by indirect effects of dUMP arising from destabilization of the template-primer, which increased strand slippage and realignment errors during polymerization. Similar observations with reverse transcription now suggest this proposed effect of dUMP may be general.

A further aspect of interpreting the mutational spectrum that arises during dUMP incorporation is whether the errors occur during minus strand or plus strand synthesis. Two

observations that favor a predominantly minus strand error mechanism are (i) the known lower fidelity of reverse transcriptase when using an RNA template [43], and (ii) the complete absence of base mismatches detected during DNA sequencing (for instance, an original G/U base mismatch should yield Sanger strand reads consisting of a mixture of G/C and A/T at that site after PCR amplification). The occurrence of predominantly minus strand errors is suggested because a mismatch generated during (-) strand synthesis would always be removed during degradation of the plus strand RNA by HIV RNaseH, whereas mismatches occurring during plus strand synthesis would remain. Although DNA repair could repair plus strand mismatches, the low repair capacity of nondividing cells makes this unlikely compared to the simple minus strand mechanism. Consistent with this idea, a recent deep sequencing study concluded that minus strand deamination events catalyzed by A3G were only inefficiently repaired by UBER or mismatch repair in T cells, which have much greater repair activity than MDM [44].

Conclusions

These in vitro results inform on the previous detection of dUMP in both alveolar macrophages and peripheral blood monocytes of HIV patients on ART [4]. We find that the kinetics for MC infection is compatible with their lifetime *in vivo* and their near absence of hUNG2 activity is consistent with the retention of viral dUMP at high levels at least until differentiation into macrophages, where UBER becomes possible. Thus, the fate of uracilated proviruses would appear to center on the expression levels of UBER enzymes in different cellular environments and whether infected macrophages can enter the repair competent G_1 state. A full understanding of these complexities in the context of *in vivo* derived macrophages is therefore essential. Our current understanding suggests that potential therapeutic opportunities may exist for eradicating densely uracilated proviruses if UBER could be activated under conditions where subsequent repair is interrupted pharmacologically.

Supporting information

S1 Methods. Supplemental methods. RT-PCR measurements of T cell receptor RNA, single nucleotide polymerase extension assay, western Blotting, measurement of mRNA expression levels of UBER enzymes using RT-qPCR, uracil content of viral DNA, RT-qPCR of extracellular viral RNA, activity of HIV reverse transcriptase with dUTP and dTTP substrates, sequencing of single viral reverse transcripts and genomic RNA copies, over-expression of hUNG in MDMs, gel-based hUNG activity assay.
(DOCX)

S1 Fig. Measurement of dTTP and dUTP levels in the Hap1 dividing cell line. The single nucleotide extension assay was used to establish the differences in dUTP/dTTP between MDM, MC and HAP1 dividing cells. The procedure is described in Methods. (a) Denaturing urea-PAGE of extension reactions in the presence and absence of dUTPase. The fold serial dilution of the dNTP extract used in each reaction is shown above each lane and establishes that the extension reaction is within the linear range of the assay (0.05–0.9 fraction substrate extended). The total [dTTP + dUTP] pool was 68 ± 6 pmol/million cells which was comprised entirely of dTTP (64 ± 4 pmol/million cells). (b) Single nucleotide extension reactions using cell extracts from monocytes (donor 2). The image is from one of two replicate measurements. Control reactions included polymerase in the absence and presence of added [dUTP + dNTPs] and dUTPase.
(DOCX)

S2 Fig. Determination of hUNG2 activity in extracts from Hap 1 cells and UBER mRNA expression levels in MDMs and comparison with the HAP1 dividing cell line. (a) Fluorometric activity assay for hUNG2 activity in Hap1 cell extracts (red data)(10 μg of total cell extract protein was used in the assay, see Methods). The a linear regression line through the data points is shown. The hUNG2 activity in Hap1 dividing cells is at least 25-fold greater than MDM and MC. For comparison, the black dashed line shows the equivalent activity present in MDM/MC as shown in Fig 2 of the main text. (b) mRNA expression levels of UBER enzymes in MDM relative to HAP1 dividing cells. Total RNA was extracted from MDMs after seven days differentiation from MC. The error bars in the qPCR measurements show the standard deviation from three replicate measurements.
(DOCX)

S3 Fig. Morphological and granulation differences between MDMs and MCs. (a) Flow cytometry analysis of monocytes immediately after purification. (b) Flow cytometry analysis of monocytes cultured in suspension under non-adherent conditions for seven days. (c) Flow cytometry analysis of fully differentiated MDM (cultured for 7 days under adherent conditions in the presence of M-CSF). (d) Light microscope image of monocytes immediately after purification (20x magnification, 5x zoom). (e) Light microscope image of monocytes after 7 days of culture under non-adherent conditions in the absence of M-CSF (20x magnification, 5x zoom). (f) Light microscope image MDM after 7 days of culture in the presence of M-CSF (20x magnification, 4x image reduction.
(DOCX)

S4 Fig. HIV-eGFP expression in MC and MDM. (a) MC were infected with HIV$^{NL4-3(eGFP)}$ immediately after isolation at an MOI of ten. At 7-days post infection, eGFP expression was measured by flow cytometry. Even though GFP fluorescence is very low, viral reverse transcripts are abundant (main text). (b) Fully differentiated MDM were infected with HIV$^{NL4-3(eGFP)}$ at an MOI of ten. At 7-days post infection, eGFP expression was measured by flow cytometry.
(DOCX)

S5 Fig. Activity of lentiviral transduced hUNG2 in MDM cell extracts under uninduced and induced conditions. MDM were transduced with a lentiviral construct containing full length hUNG2 (pCW.57.1.FL.UNG) at MOI of 5 (0.1 pg p24/cell). Total cell extracts were prepared at days 1 and 3 post-transduction and protein concentrations were determined by the Bradford assay. hUNG activity in cell extracts was determined by gel-based UNG activity assay using equal amounts of total protein and a 19-mer uracil-containing ssDNA substrate with a FAM label on the 5′-end (see Methods). Excision of uracil results in a 5′-FAM labeled 9mer product band.
(DOCX)

S6 Fig. Effect of over expression of hUNG2 in MDMs on total HIV DNA. Fully differentiated MDM were first transduced with inducible lentiviral construct expressing full length hUNG at an MOI of 5 (0.1 pg p24/cell) and 3 days later induced with doxycycline (1ug/ml). 1-day after induction, MDM were then infected with HIV^{NL4-3} single round virus at MOI of 0.5 (0.05 pg p24/cell). Total DNA was extracted at days 1, 3 and 7 and (a) LRT copies and (b) Frac U were measured by Ex-qPCR.
(DOCX)

S1 Table. Primer and molecular beacon probe sequences for viral DNA sequences and RT-PCR measurements of UBER enzyme mRNA expression (5'→3').
(DOCX)

S2 Table. Clonal mutation analysis of HIV proviral DNA isolated from infected MDM at 7 dpi.
(DOCX)

S3 Table. Clonal mutation analysis of HIV proviral DNA isolated from infected MC at 7 dpi.
(DOCX)

S4 Table. Clonal mutation analysis of dUMP-depleted HIV proviral DNA isolated from infected MDM at 7 dpi.
(DOCX)

S5 Table. Clonal mutation analysis of extra cellular viral RNA extracted from infected MDM culture supernatants at 7 dpi[a].
(DOCX)

S1 Raw Image.
(DOCX)

Acknowledgments

Author Contributions

Conceptualization: Mesfin Meshesha, James T. Stivers.

Data curation: Mesfin Meshesha, Alexandre Esadze.

Formal analysis: Mesfin Meshesha, Alexandre Esadze, Junru Cui, Natela Churgulia, James T. Stivers.

Funding acquisition: James T. Stivers.

Investigation: Mesfin Meshesha, Alexandre Esadze, Junru Cui, Natela Churgulia, Sushil Kumar Sahu.

Methodology: Mesfin Meshesha, Alexandre Esadze, Junru Cui, Natela Churgulia, James T. Stivers.

Project administration: James T. Stivers.

Resources: James T. Stivers.

Supervision: James T. Stivers.

Validation: Mesfin Meshesha, Alexandre Esadze, Junru Cui, Natela Churgulia, James T. Stivers.

Visualization: James T. Stivers.

Writing – original draft: Mesfin Meshesha, Alexandre Esadze, Junru Cui, James T. Stivers.

Writing – review & editing: Mesfin Meshesha.

References

1. Gandhi SK, Siliciano JD, Bailey JR, Siliciano RF, Blankson JN. Role of APOBEC3G/F-Mediated Hypermutation in the Control of Human Immunodeficiency Virus Type 1 in Elite Suppressors. J Virol. 2008; 82:3125–30. https://doi.org/10.1128/JVI.01533-07 PMID: 18077705

2. Harris RS, Dudley JP. APOBECs and virus restriction. Virology. 2015; 479–480:131–45. https://doi.org/10.1016/j.virol.2015.03.012 PMID: 25818029

3. Weil AF, Ghosh D, Zhou Y, Seiple L, McMahon MA, Spivak AM, et al. Uracil DNA glycosylase initiates degradation of HIV-1 cDNA containing misincorporated dUTP and prevents viral integration. Proc Natl Acad Sci U S A. 2013; 110:E448–57. https://doi.org/10.1073/pnas.1219702110 PMID: 23341616

4. Hansen EC, Ransom M, Hesselberth JR, Hosmane NN, Capoferri AA, Bruner KM, et al. Diverse fates of uracilated HIV-1 DNA during infection of myeloid lineage cells. Elife [Internet]. 2016; 5. Available from: http://dx.doi.org/10.7554/eLife.18447

5. Priet S, Gros N, Navarro J-M, Boretto J, Canard B, Quérat G, et al. HIV-1-associated uracil DNA glycosylase activity controls dUTP misincorporation in viral DNA and is essential to the HIV-1 life cycle. Mol Cell. 2005; 17:479–90. https://doi.org/10.1016/j.molcel.2005.01.016 PMID: 15721252

6. Yan N, O'Day E, Wheeler LA, Engelman A, Lieberman J. HIV DNA is heavily uracilated, which protects it from autointegration. Proc Natl Acad Sci U S A. 2011; 108:9244–9. https://doi.org/10.1073/pnas.1102943108 PMID: 21576478

7. Vértessy BG, Tóth J. Keeping uracil out of DNA: physiological role, structure and catalytic mechanism of dUTPases. Acc Chem Res. 2009; 42:97–106. https://doi.org/10.1021/ar800114w PMID: 18837522

8. Priet S, Sire J, Quérat G. Uracils as a cellular weapon against viruses and mechanisms of viral escape. Curr HIV Res. 2006; 4:31–42. https://doi.org/10.2174/157016206775197673 PMID: 16454709

9. Cui J, Gizzi A, Stivers JT. Deoxyuridine in DNA has an inhibitory and promutagenic effect on RNA transcription by diverse RNA polymerases. Nucleic Acids Res. 2019; 47:4153–68. https://doi.org/10.1093/nar/gkz183 PMID: 30892639

10. Zhang H, Yang B, Pomerantz RJ, Zhang C, Arunachalam SC, Gao L. The cytidine deaminase CEM15 induces hypermutation in newly synthesized HIV-1 DNA. Nature. 2003; 424:94–8. https://doi.org/10.1038/nature01707 PMID: 12808465

11. Amie SM, Noble E, Kim B. Intracellular nucleotide levels and the control of retroviral infections. Virology. 2013; 436:247–54. https://doi.org/10.1016/j.virol.2012.11.010 PMID: 23260109

12. Gavegnano C, Kennedy EM, Kim B, Schinazi RF. The Impact of Macrophage Nucleotide Pools on HIV-1 Reverse Transcription, Viral Replication, and the Development of Novel Antiviral Agents. Mol Biol Int. 2012; 2012:625983. https://doi.org/10.1155/2012/625983 PMID: 22811909

13. Eldin P, Chazal N, Fenard D, Bernard E, Guichou J-F, Briant L. Vpr expression abolishes the capacity of HIV-1 infected cells to repair uracilated DNA. Nucleic Acids Res. 2014; 42:1698–710. https://doi.org/10.1093/nar/gkt974 PMID: 24178031

14. Ahn J, Vu T, Novince Z, Guerrero-Santoro J, Rapic-Otrin V, Gronenborn AM. HIV-1 Vpr loads uracil DNA glycosylase-2 onto DCAF1, a substrate recognition subunit of a cullin 4A-ring E3 ubiquitin ligase for proteasome-dependent degradation. J Biol Chem. 2010; 285:37333–41. https://doi.org/10.1074/jbc.M110.133181 PMID: 20870715

15. Schröfelbauer B, Yu Q, Zeitlin SG, Landau NR. Human immunodeficiency virus type 1 Vpr induces the degradation of the UNG and SMUG uracil-DNA glycosylases. J Virol. 2005; 79:10978–87. https://doi.org/10.1128/JVI.79.17.10978-10987.2005 PMID: 16103149

16. Langevin C, Maidou-Peindara P, Aas PA, Jacquot G, Otterlei M, Slupphaug G, et al. Human immunodeficiency virus type 1 Vpr modulates cellular expression of UNG2 via a negative transcriptional effect. J Virol. 2009; 83:10256–63. https://doi.org/10.1128/JVI.02654-08 PMID: 19625402

17. Rogstad DK, Liu P, Burdzy A, Lin SS, Sowers LC. Endogenous DNA lesions can inhibit the binding of the AP-1 (c-Jun) transcription factor. Biochemistry. 2002; 41:8093–102. https://doi.org/10.1021/bi012180a PMID: 12069602

18. Sonza S, Mutimer HP, Oelrichs R, Jardine D, Harvey K, Dunne A, et al. Monocytes harbour replication-competent, non-latent HIV-1 in patients on highly active antiretroviral therapy. AIDS. 2001; 15:17–22. https://doi.org/10.1097/00002030-200101050-00005 PMID: 11192864

19. Calcaterra S, Cappiello G, Di Caro A, Garbuglia AR, Benedetto A. Comparative analysis of total and integrated HIV-1 DNA in peripheral CD4 lymphocytes and monocytes after long treatment with HAART. J Infect. 2001; 43:239–45. https://doi.org/10.1053/jinf.2001.0875 PMID: 11869061

20. Ziegler-Heitbrock L. Reprint of: Monocyte subsets in man and other species. Cell Immunol. 2014; 291:11–5. https://doi.org/10.1016/j.cellimm.2014.06.008 PMID: 25015741

21. Crowe S, Zhu T, Muller WA. The contribution of monocyte infection and trafficking to viral persistence, and maintenance of the viral reservoir in HIV infection. 2017; 74:635–41.

22. Nottet HS, Persidsky Y, Sasseville VG, Nukuna AN, Bock P, Zhai QH, et al. Mechanisms for the trans-endothelial migration of HIV-1-infected monocytes into brain. J Immunol. 1996; 156:1284–95. PMID: 8558009

23. Persidsky Y, Stins M, Way D, Witte MH, Weinand M, Kim KS, et al. A model for monocyte migration through the blood-brain barrier during HIV-1 encephalitis. J Immunol. 1997; 158:3499–510. PMID: 9120312

24. Kennedy EM, Daddacha W, Slater R, Gavegnano C, Fromentin E, Schinazi RF, et al. Abundant non-canonical dUTP found in primary human macrophages drives its frequent incorporation by HIV-1 reverse transcriptase. J Biol Chem. 2011; 286:25047–55. https://doi.org/10.1074/jbc.M111.234047 PMID: 21454906

25. Bauer M, Goldstein M, Christmann M, Becker H, Heylmann D, Kaina B. Human monocytes are severely impaired in base and DNA double-strand break repair that renders them vulnerable to oxidative stress. Proceedings of the National Academy of Sciences. 2011; 108:21105–10.

26. O'Doherty U, Swiggard WJ, Jeyakumar D, McGain D, Malim MH. A sensitive, quantitative assay for human immunodeficiency virus type 1 integration. J Virol. 2002; 76:10942–50. https://doi.org/10.1128/jvi.76.21.10942-10950.2002 PMID: 12368337

27. Mlcochova P, Sutherland KA, Watters SA, Bertoli C, de Bruin RAM, Rehwinkel J, et al. A G1-like state allows HIV-1 to bypass SAMHD1 restriction in macrophages. EMBO J. John Wiley & Sons, Ltd; 2017; 36:604–16. https://doi.org/10.15252/embj.201696025 PMID: 28122869

28. Lichtenstein DL, Rushlow KE, Cook RF, Raabe ML, Swardson CJ, Kociba GJ, et al. Replication in vitro and in vivo of an equine infectious anemia virus mutant deficient in dUTPase activity. J Virol. 1995; 69:2881–8. PMID: 7707512

29. Turelli P, Pétursson G, Guiguen F, Mornex JF, Vigne R, Quérat G. Replication properties of dUTPase-deficient mutants of caprine and ovine lentiviruses. J Virol. 1996; 70:1213–7. PMID: 8551582

30. Threadgill DS, Steagall WK, Flaherty MT, Fuller FJ, Perry ST, Rushlow KE, et al. Characterization of equine infectious anemia virus dUTPase: growth properties of a dUTPase-deficient mutant. J Virol. 1993; 67:2592–600. PMID: 8386267

31. Steagall WK, Robek MD, Perry ST, Fuller FJ, Payne SL. Incorporation of uracil into viral DNA correlates with reduced replication of EIAV in macrophages. Virology. 1995; 210:302–13. https://doi.org/10.1006/viro.1995.1347 PMID: 7542416

32. Mansky LM, Preveral S, Selig L, Benarous R, Benichou S. The interaction of vpr with uracil DNA glyco-sylase modulates the human immunodeficiency virus type 1 In vivo mutation rate. J Virol. 2000; 74:7039–47. https://doi.org/10.1128/jvi.74.15.7039-7047.2000 PMID: 10888643

33. Guenzel CA, Hérate C, Le Rouzic E, Maidou-Peindara P, Sadler HA, Rouyez M-C, et al. Recruitment of the nuclear form of uracil DNA glycosylase into virus particles participates in the full infectivity of HIV-1. J Virol. 2012; 86:2533–44. https://doi.org/10.1128/JVI.05163-11 PMID: 22171270

34. Meyerhans A, Vartanian JP, Hultgren C, Plikat U, Karlsson A, Wang L, et al. Restriction and enhance-ment of human immunodeficiency virus type 1 replication by modulation of intracellular deoxynucleoside triphosphate pools. J Virol. 1994; 68:535–40. PMID: 8254768

35. Diamond TL, Roshal M, Jamburuthugoda VK, Reynolds HM, Merriam AR, Lee KY, et al. Macrophage tropism of HIV-1 depends on efficient cellular dNTP utilization by reverse transcriptase. J Biol Chem. 2004; 279:51545–53. https://doi.org/10.1074/jbc.M408573200 PMID: 15452123

36. Brown A, Zhang H, Lopez P, Pardo CA, Gartner S. In vitro modeling of the HIV-macrophage reservoir. J Leukoc Biol. 2006; 80:1127–35. https://doi.org/10.1189/jlb.0206126 PMID: 16923921

37. Cromer D, Schlub TE, Smyth RP, Grimm AJ, Chopra A, Mallal S, et al. HIV-1 Mutation and Recombina-tion Rates Are Different in Macrophages and T-cells. Viruses. 2016; 8:118. https://doi.org/10.3390/v8040118 PMID: 27110814

38. Curlin ME, Zioni R, Hawes SE, Liu Y, Deng W, Gottlieb GS, et al. HIV-1 envelope subregion length vari-ation during disease progression. PLoS Pathog. 2010; 6:e1001228. https://doi.org/10.1371/journal.ppat.1001228 PMID: 21187897

39. Zolla-Pazner S, Cardozo T. Structure-function relationships of HIV-1 envelope sequence-variable regions refocus vaccine design. Nat Rev Immunol. 2010; 10:527–35. https://doi.org/10.1038/nri2801 PMID: 20577269

40. Carr CE, Khutsishvili I, Gold B, Marky LA. Thermodynamic Stability of DNA Duplexes Comprising the Simplest T → dU Substitutions. Biochemistry. 2018; 57:5666–71. https://doi.org/10.1021/acs.biochem.8b00676 PMID: 30185020

41. Parker JB, Stivers JT. Dynamics of uracil and 5-fluorouracil in DNA. Biochemistry. 2011; 50:612–7. https://doi.org/10.1021/bi101536k PMID: 21190322

42. Wärmländer S, Sponer JE, Sponer J, Leijon M. The Influence of the Thymine C5 Methyl Group on Spontaneous Base Pair Breathing in DNA. J Biol Chem. 2002; 277:28491–7. https://doi.org/10.1074/jbc.M202989200 PMID: 12029089

43. Abram ME, Ferris AL, Shao W, Alvord WG, Hughes SH. Nature, Position, and Frequency of Mutations Made in a Single Cycle of HIV-1 Replication. J Virol. 2010; 84:9864–78. https://doi.org/10.1128/JVI. 00915-10 PMID: 20660205

44. Pollpeter D, Parsons M, Sobala AE, Coxhead S, Lang RD, Bruns AM, et al. Deep sequencing of HIV-1 reverse transcripts reveals the multifaceted antiviral functions of APOBEC3G. Nat Microbiol. 2018; 3:220–33. https://doi.org/10.1038/s41564-017-0063-9 PMID: 29158605